Protein mobility and diffusive barriers in Escherichia coli

Bogaart, Geert van den; Hermans, Nicolaas; Krasnikov, Viktor; Poolman, Bert

Published in:
Molecular Microbiology

DOI:
10.1111/j.1365-2958.2007.05705.x

Publication date:
2007

Molecular Microbiology (2007) **64**(3), 858–871 doi:10.1111/j.1365-2958.2007.05705.x

Protein mobility and diffusive barriers in *Escherichia coli*: consequences of osmotic stress

Geert van den Bogaart,[1] Nicolaas Hermans,[1] Victor Krasnikov[2] and Bert Poolman[1]*
[1]*Biochemistry Department and* [2]*Ultrafast Laser and Spectroscopy Laboratory, Groningen Biomolecular Science and Biotechnology Institute and Zernike Institute for Advanced Materials, University of Groningen, the Netherlands.*

Summary

The effect of osmotic stress on the intracellular diffusion of proteins in *Escherichia coli* was studied, using a pulsed version of fluorescence recovery after photo-bleaching, pulsed-FRAP. This method employs sequences of laser pulses which only partly bleach the fluorophores in a cell. Because the cell size and geometry are taken into account, pulsed-FRAP enables to measure diffusion in very small cells of different shapes. We found that upon an osmotic upshock from 0.15 to 0.6 Osm, imposed by NaCl or sorbitol, the apparent intracellular diffusion (*D*) of mobile green fluorescent protein (GFP) decreased from 3.2 to 0.4 $\mu m^2 s^{-1}$, whereas the membrane permeable glycerol had no effect. Exposing *E. coli* cells to higher osmolalities (> 0.6 Osm) led to compartmentalization of the GFP into discrete pools, from where the GFP could not escape. Although free diffusion through the cell was hindered, the mobility of GFP in these pools was still relatively high (*D* ~0.4 $\mu m^2 s^{-1}$). The presence of osmoprotectants restored the effect of osmotic stress on the protein mobility and apparent compartmentalization. Also, lowering the osmolality from 0.6 Osm back to 0.15 Osm restored the mobility of GFP. The implications of these findings in terms of heterogeneities and diffusive barriers inside the cell are discussed.

Introduction

Bacterial cells are very crowded with biomacromolecules. In *Escherichia coli* the concentration of proteins, DNA and RNA is 200–320 mg ml^{-1} (Cayley *et al*., 1991; Zimmerman and Trach, 1991) and the macromolecules account for ~25–30% of the cell volume (Cayley and Record, 2004). Upon an osmotic shock, the concentration of macromolecules can increase up to 400 mg ml^{-1}, but the cells remain viable (Cayley *et al*., 1991; Cayley and Record, 2004). This concentration is approaching that of a protein crystal, and in hyperosmotically stressed bacteria the macromolecules can account for ~50% of the cell volume. Approximating the macromolecules as 5 nm diameter spheres, the surface to surface distances of the molecules become less than 1 nm (Spitzer and Poolman, 2005). At these small distances, the high cytoplasmic crowding has been proposed to shape the cell volume into transient networks of electrolyte pathways and pools, enabling a flow of biochemical ions through the cytoplasm (Spitzer and Poolman, 2005). The steric hindrance and electrostatic effects will have a significant impact on the mobility of proteins in the cytoplasm (Ellis, 2001; Cayley and Record, 2004).

Fluorescence recovery after photo-bleaching (FRAP) has been used to study green fluorescent protein (GFP) mobility *in vivo* in eukaryotic cells (Swaminathan *et al*., 1997) and various organelles (see Lippincott-Schwartz *et al*., 2003 for a review). In bacteria, FRAP was first applied to measure protein diffusion in *E. coli* by Elowitz *et al*. (1999) and later by Mullineaux *et al*. (2006). Recently, Konopka *et al*. (2006) used FRAP to study the effect of osmotic stress on the intracellular diffusion of GFP. With FRAP, a spot is irreversibly photo-bleached by a brief intense light pulse. Using an attenuated probe beam, the diffusion of unbleached fluorophores into the photo-bleached area is then measured. The recovery of the fluorescence over time is proportional to the mobility of the fluorophore. However, FRAP measurements on prokaryotic cells and cell organelles are technically difficult due to their small size, which is close to the best achievable optical resolution. Thus, unlike in large eukaryotic cells, in prokaryotic cells a very large fraction (> 40% in the published studies) of fluorophore is photo-bleached and this leads to incomplete recovery. Also, diffusion is affected by the proximity of the cell membrane. To deal with these problems, one can collect series of cell images during the recovery process and thereby take the whole GFP content and geometry into account (Elowitz *et al*., 1999; Konopka *et al*., 2006; Mullineaux *et al*., 2006).

Here, we report on a new approach to overcome the problem of photo-bleaching of a large fraction of fluorophores in a small cell. Instead of using a separate bleach-

Accepted 16 March, 2007. *For correspondence. E-mail B.Poolman@rug.nl; Tel. (+31) 50 3634190; Fax (+31) 50 3634165.

ing and probe beam, we use sequences of short, low intensity (1 s, < 1 kW cm^{-2}) laser pulses (pulsed-FRAP). For the data analysis, we take into account both the kinetics of photo-bleaching and the end level of recovery, hence combining continuous photo-bleaching with FRAP. Like FRAP, continuous photo-bleaching has been used to measure the diffusion constant in vesicles and cells (Delon *et al.*, 2006 and references therein). With continuous photo-bleaching, the fluorescence decay is fitted with a model that incorporates the rate of photo-bleaching and the diffusion coefficient. To deal with the geometry of the cell, we determine the shape of the bacterium and use a numerical finite difference method to approximate the diffusion/photo-bleaching rates. Because the cell size and geometry are taken into account, pulsed-FRAP can be used to probe protein mobility in small compartments of various shapes. With pulsed-FRAP, only the fraction of GFP located in the focal volume is measured rather than the distribution in the cell as a whole, which, as we will show in this article, can reveal macromolecular heterogeneities that are not readily observed by other methods. Moreover, it can be used to probe the mobility of very photo-instable fluorophores. Pulsed-FRAP may find applications in probing (macro)molecule mobility in small bacteria and eukaryotic cell organelles.

Results

Principle of pulsed-FRAP

Escherichia coli cells expressing GFP at a relatively low level were grown to mid-exponential phase to measure the diffusion of this fluorescent molecule in the cell. Under the microscope, no inclusion bodies were visible. The cells were then washed and resuspended in low osmolality (0.15 Osm) medium consisting of 25 mM Na-phosphate, pH 7.0, supplemented with 50 mM glucose, to remove K^+ present in the growth medium. K^+ ions were removed to prevent an active response of the cells to an osmotic shock through the accumulation of this ion (see below). The intracellular protein diffusion was measured using the following protocol. First, an *E. coli* cell expressing GFP was imaged with a laser-scanning confocal microscope, after which the laser beam was blocked with a shutter and focused in the centre of the cell [Fig. 1A, left panel, position (i_0, j_0)]. Then, the shutter was opened to record the decay in fluorescence for 1 s (Fig. 1B, from t_0 to t_1), and, subsequently, the shutter was closed for 3–100 s and the fluorescence recovery (at t_2) was measured. Depending on the physiological conditions (extent of osmotic stress), the mobility of GFP differed and this required shorter or longer periods of shutter closing to allow the fluorescence in the focal volume to reach a new steady state (before a new pulse of light could be applied). After the measurements, the cells were imaged again and a computational grid was superimposed over the confocal image (Fig. 1A, left panel). The diffusion constant and bleaching rate were obtained by approximating the photobleaching and spatial redistribution of GFP with a numerical finite difference method as described in *Experimental procedures*.

For unshocked cells, the GFP was uniformly spatially distributed over the cell before and < 1 s after photobleaching, in accordance with literature data (Elowitz *et al.*, 1999; Konopka *et al.*, 2006; Mullineaux *et al.*, 2006). The fluorescence was measured with an integration time of 10 ms. For each single cell measurement, the open – close cycle of the shutter was repeated 5–15 times. During the exposure time about 10–40% of the GFP situated in the confocal volume was bleached (Fig. 1B). The degree of photo-bleaching depended on the bleaching rate, the diffusion constant and the cell size. The cells were still able to divide after the measurements (not shown). The inset of Fig. 2 shows a confocal image of a cell of approximately 4 μm in length, and the main figure presents the pulsed-FRAP measurements and the fits. For unshocked cells, a diffusion constant of 3.2 $\mu m^2\ s^{-1}$ was found ($n = 64$), although the spread was broad and diffusion constants varied from 0.1 to 24 $\mu m^2\ s^{-1}$. At the laser intensity used, the bleaching rate was 3.5 ± 1.4 s^{-1} and this variation is likely due to differences in the microenvironment of the cell. No correlation of the intermediate times with the bleaching rates and diffusion constants was found, both indicating that the intervals were long enough to reach steady state conditions. Assuming the cells to be rod-shaped, the cell volume could be estimated from the confocal images and was 2.9 ± 1.3 fl for unshocked cells. The diffusion constant did not correlate with (i) the photo-bleaching rate (Fig. 3A) (ii) the expression level of GFP (Fig. 3B) and (iii) the cell volume (Fig. 3C). The cell diameter for unshocked cells was 1.0 ± 0.3 μm and did not correlate with the diffusion constant (not shown). Measurements could be made in cells as small as ~1 μm. The contribution to the fluorescence recovery of triplet state processes was insignificant, as could be seen from the 'noise' in the fluorescence traces (Figs 1B and 2). Also, triplet state processes occur at timescales << 1 s, and lastly, at high osmotic stress, the fluorescence recovery after 1 s interval time was less than 10% of the total recovery. The bleaching constant was linearly related to the laser power (not shown).

Validation of the pulsed-FRAP method

Multiple measurements at the same position in a bacterium indicated that the typical error of pulsed-FRAP was ~75%. To obtain a further estimate of the accuracy of the pulsed-FRAP method, liposomes encapsulated with GFP

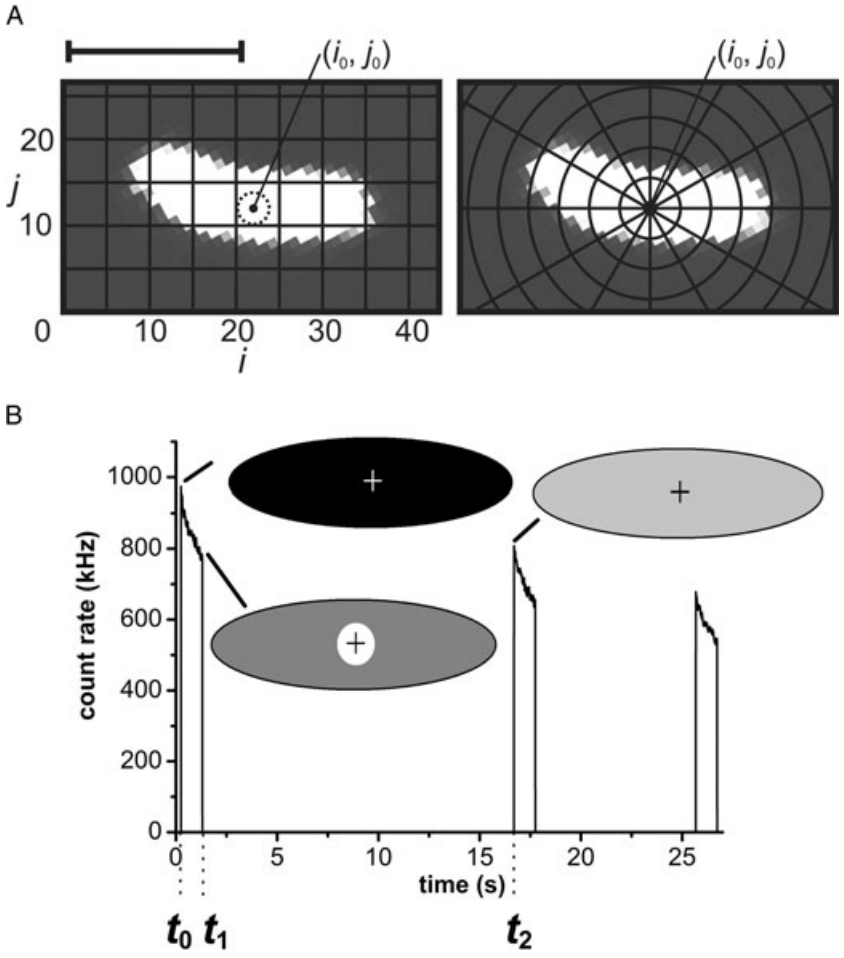

Fig. 1. Principle of pulsed-FRAP.
A. Left panel: Confocal image of an *E. coli* cell with a computational grid superimposed. The grid spacing r_s is 100 nm and the size (at ω, dotted circle) of the focused laser [position (i_0, j_0)] is indicated. The scale bar is 3 μm. Right panel: Confocal image analysis to quantify the spatial distribution of GFP. For each point located in the bacterium, the fluorescence ratios before and after the pulsed-FRAP measurement were calculated and plotted as a function of the distance from the focused laser.
B. The confocal volume is positioned on an *E. coli* cell expressing GFP and at t_0 a laser pulse of 1 s (till t_1) is applied. This results in a non-uniform spatial distribution of GFP in the cell at t_1. After a certain time interval, at t_2, the GFP distribution of the cell is homogenous again and another laser pulse of 1 s is applied. The fluorescence count rates depend on the diffusion constant D of GFP inside the cell. Only the first three of 5–15 laser pulses are shown.

were used. A cytosolic extract from *E. coli* cells expressing GFP was isolated and mixed with a concentrated polyethylene glycol 6000 (PEG6000) solution to mimic the high (macro)molecular crowding inside a cell. The diffusion constant of GFP in this mixture was measured with fluorescence correlation spectroscopy (FCS) and was $0.9 \pm 0.3\ \mu m^2\ s^{-1}$, corresponding to a viscosity of ~90 mPa s. The cytosol/PEG6000 mixture was encapsulated into μm-sized liposomes as described in (Pautot *et al*., 2003; Noireaux and Libchaber, 2004) and pulsed-FRAP measurements were performed. With pulsed-FRAP measurements, a diffusion constant of $0.4 \pm 0.3\ \mu m^2\ s^{-1}$ ($n = 18$) was found (Fig. 4) and a bleaching rate of $4.9 \pm 2.8\ s^{-1}$. The diffusion constants ranged from 0.1 to $0.7\ \mu m^2\ s^{-1}$. The absolute values and spread of the diffusion constants in these μm-sized liposomes are in reasonable agreement with the estimates of GFP mobility in the crowded cytosol/PEG6000 solutions, determined by FCS. Taken together, the spread in the diffusion constants of GFP in the cytoplasm of *E. coli* was much larger than can be expected based on the typical error of the method

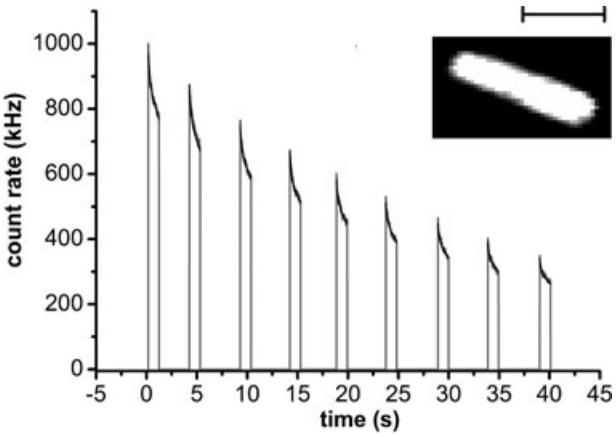

Fig. 2. Typical pulsed-FRAP traces (grey) and fit (black) from an unstressed *E. coli* cell. The inset shows the confocal image of the cell and the scale bar is 2 μm. The recording of a confocal image of this size and resolution took ~2.5 s on our setup and resulted in photobleaching of < 10% of the total GFP in the cell. The diffusion constant for this measurement was $1.8\ \mu m^2\ s^{-1}$ and the bleaching rate was $3.5\ s^{-1}$.

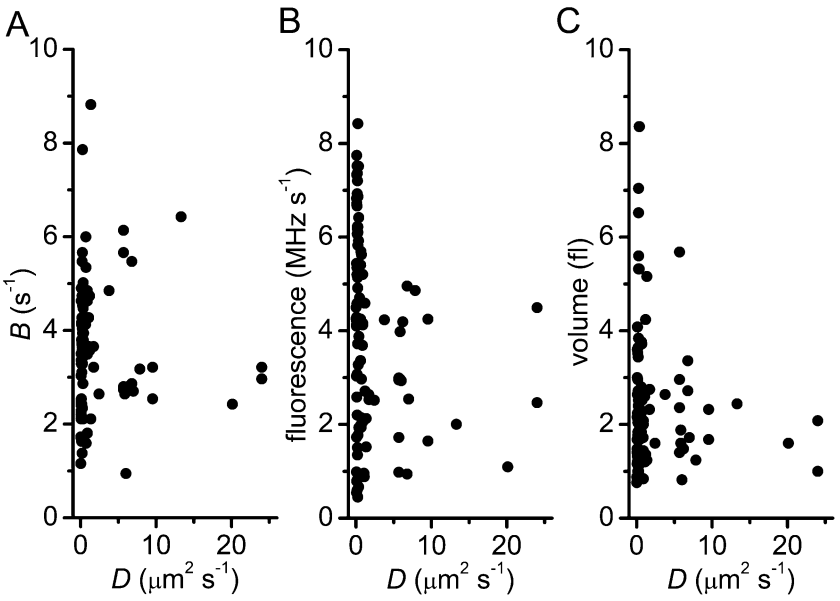

Fig. 3. Analysis of pulsed-FRAP measurements. The diffusion constant *D* did not show any apparent correlation with the photo-bleaching rate *B* (A), the initial fluorescence (corresponding to the GFP expression level, B) and the cell volume (C).

(Table 1). This indicates that the variation of the diffusion constants is to a large extent due to true variation in the sample. Mobility measurements by FCS in liposomes (and cells) of only a few μm proved far less accurate than pulsed-FRAP because of the high degree of photobleaching of GFP diffusing in such small confined spaces (not shown).

As a final control, pulsed-FRAP measurements were performed on cephalexin-treated cells, ranging in length from 4 to 16 μm. Cephalexin is a β-lactam antibiotic that inhibits penicillin-binding protein 3 and impairs cell division (Eberhardt *et al*., 2003), resulting in long cell filaments (Ishihara *et al*., 1983) that are more suitable for conventional FRAP measurements. In cephalexin-treated cells, an average diffusion constant of 9.8 ± 3.6 $\mu m^2 s^{-1}$ ($n = 25$) was found. The cephalexin-treated cells were very fragile and sensitive to osmotic stress (Starka, 1971; Fischer, 1989; G. van den Bogaart *et al*., unpubl. result) and still formed partial septa, which might influence the diffusion of proteins in the cytosol. For studying physiologically relevant parameters related to osmotic stress, the filamentous cells were not very suited and not used further.

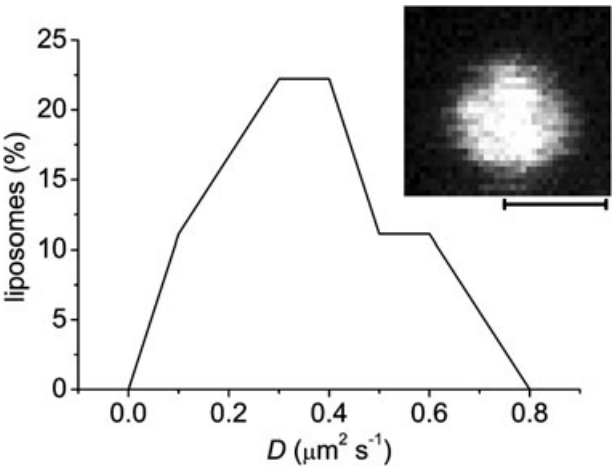

Fig. 4. Pulsed-FRAP measurements in liposomes. A cytosolic fraction from *E. coli* cells, expressing GFP, was extracted and mixed 1:1 with 400 g PEG6000 kg^{-1} milli-Q; the final protein concentration was 20 mg ml^{-1}. The diffusion of GFP in this crowded mixture was 0.9 ± 0.3 $\mu m^2 s^{-1}$ and was determined by FCS. The mixture was encapsulated in ~μm-sized liposomes (inset) and pulsed-FRAP measurements were performed. The distribution of the diffusion coefficients is shown in the main figure with a bin width of 0.1 $\mu m^2 s^{-1}$. The average diffusion was 0.4 $\mu m^2 s^{-1}$ ($n = 18$). The inset shows a confocal image of a liposome. The scale bar is 1 μm.

Osmotic stress: moderate upshock

To study the effect of an osmotic upshock on the intracellular diffusion of GFP, *E. coli* cells were exposed to increasing concentrations of NaCl. After an osmotic upshock with NaCl from 0.15 to 0.57 Osm (addition of 250 mM NaCl), the diffusion constant in the cells decreased from 3.2 to 0.4 $\mu m^2 s^{-1}$. Although in both cases the spread in the diffusion constants was broad (Fig. 5A and Table 1), the difference was significant ($P < 0.025$), using a one-sided *t*-test. Treatment with an intermediate osmolality of 0.37 Osm (addition of 125 mM NaCl) resulted in a diffusion constant of 1.8 $\mu m^2 s^{-1}$ and this was not significantly different ($P > 0.2$) from unshocked cells. The medium the unshocked cells were resuspended in had a lower osmolality (0.15 Osm) than the Luria–Bertani (LB) (0.24 Osm) in which the cells were grown. Next, we analysed the GFP mobility in cells washed and resuspended in medium of higher osmolality (0.47 Osm), con-

Table 1. Diffusion of GFP in *E. coli*.

C^a	Osm[b]	D_{GFP}[c]	range[d]	n^e	*t*-test[f]	γ^g
0	0.15	3.2	0.1–24	64		25
125 NaCl	0.37	1.8	0.1–13	18		44
250 NaCl	0.57	0.4	0.0–3.5	18	+	197
500 sorbitol	0.62	0.7	0.1–5.7	21	+	112
500 sorbitol + 10 KCl	0.64	2.0	0.2–6.8	15		39
500 sorbitol + 10 KCl + 1 betaine + 1 Pro	0.64	4.0	0.1–24	13		20
500 glycerol	0.65	2.3	0.1–21	17		34
500 glycerol + 10 KCl	0.66	3.1	0.1–17	15		25
500 glycerol + 10 KCl + 1 betaine + 1 Pro	0.66	3.0	0.2–23	15		26

a. NaCl, sorbitol, glycerol, KCl and glycine betaine (betaine) plus proline (Pro) concentrations in mM.
b. Measured osmolality in Osm.
c. Diffusion constant of GFP in $\mu m^2\ s^{-1}$.
d. Range of the diffusion constants in $\mu m^2\ s^{-1}$.
e. Number of measured cells.
f. + indicates that the diffusion constant is significantly different from unshocked cells ($C = 0$) based on a single-sided *t*-test and $P < 0.025$.
g. Apparent viscosity (γ) of the cytoplasm in mPa s.

sisting of 200 mM (instead of 25 mM) Na-phosphate, pH 7.0, plus 50 mM glucose. As anticipated, this resulted in a somewhat lower diffusion constant of 2.9 $\mu m^2\ s^{-1}$, values ranging from 0.1 to 19 $\mu m^2\ s^{-1}$. The diffusion constants measured in cells in 0.15 Osm medium and osmotically shocked with 500 mM sorbitol to 0.62 Osm are shown in Fig. 5B. Addition of sorbitol resulted in a significant decrease of the diffusion constants to 0.7 $\mu m^2\ s^{-1}$ ($P < 0.025$, one-sided *t*-test), similar to the impact of NaCl stress. The presence of 10 mM of the osmoprotectant K^+ with or without 1 mM proline plus 1 mM glycine betaine, resulted in (partial) restoration of the mobility and yielded diffusion constants of 2.0 $\mu m^2\ s^{-1}$ for K^+ and 4.0 $\mu m^2\ s^{-1}$ for K^+ plus glycine betaine and proline, both not significantly different from unshocked cells. Clearly, the combination of K^+ ions plus the organic osmoprotectants restored the diffusive properties of the cytoplasm to what they were before the osmotic upshock (both with NaCl and sorbitol as stressing agent). Exposing the cells to hyperosmotic conditions with the membrane-permeable sugar alcohol glycerol did not alter the diffusion constant of cytoplasmic GFP (not shown).

Osmotic stress: large upshock

When *E. coli* was exposed to osmolalities higher than 0.6 Osm (NaCl > 250 mM), a fraction of the GFP became immobile in ~75% of the cells at 1.32 Osm and 100% of the cells at >1.84 Osm. To quantify the fraction of immobile GFP, the percentage of the fluorescence intensity after the pulsed-FRAP measurement was plotted as a function of distance to the focused laser beam (Fig. 1A, right panel). Figure 6A shows these curves for three typical cells exposed to 0, 250 and 500 mM of NaCl (0.15,

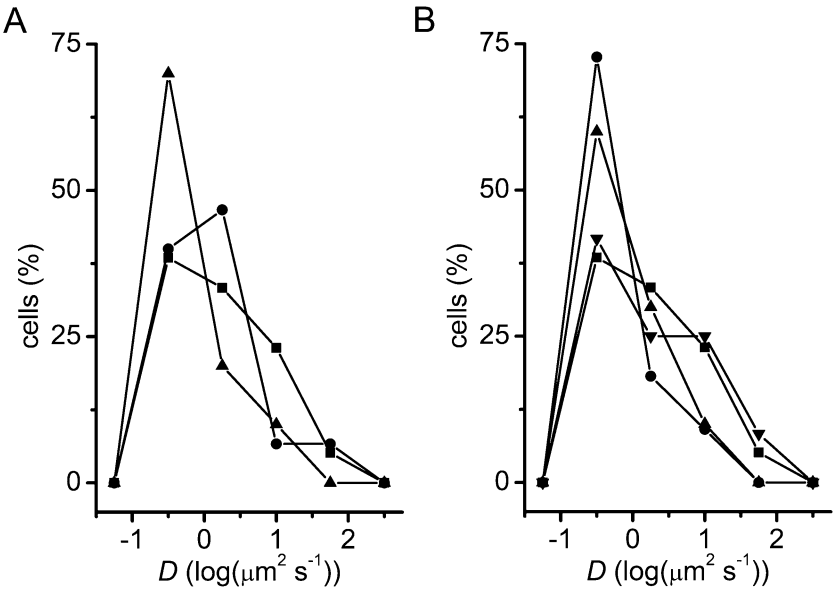

Fig. 5. The effect of osmotic stress on the intracellular diffusion of GFP.
A. The distribution of cells as a function of the diffusion constant for unstressed cells at 0.15 Osm (■) and cells stressed with NaCl to 0.37 Osm (●) and 0.57 Osm (▲).
B. The distribution of cells as a function of the diffusion constant for unstressed cells at 0.15 Osm (■), and sorbitol-treated cells at 0.62 Osm, in the absence (●) or presence of 10 mM KCl (▲), or 10 mM KCl plus 1 mM glycine betaine and 1 mM proline (▼). For plotting of the data, the cells were pooled with bin width $\log(D_1/D_2) = 0.75$.

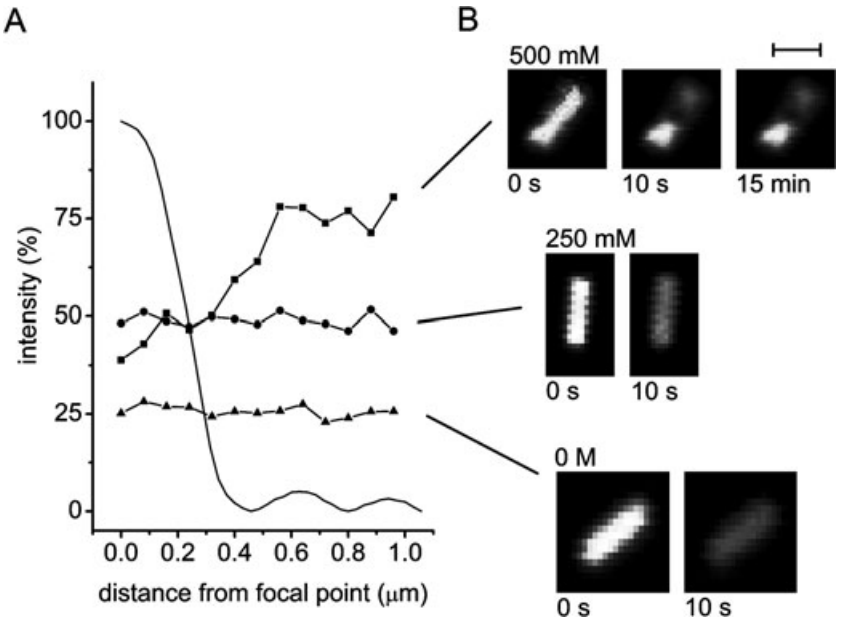

Fig. 6. A. Fluorescence intensity distributions as described in Fig. 1A (right panel) for three *E. coli* cells, treated with different NaCl concentrations: 0.15 Osm (0 M, ▲), 0.57 Osm (250 mM, ●) and 1.32 Osm (500 mM, ■). The intensity before photo-bleaching was set to 100%. The intensity of the focused laser (Airy disk) is plotted (solid line). The bin width (80 nm) was chosen to pool a sufficient number of image pixels. Because the bin width is smaller than the diffraction limit, the fluorescence intensity changes gradually within several adjacent bins.
B. The confocal images corresponding to the curves in A, prior (0 s) and 10 s after the pulsed-FRAP measurement. The non-uniform fluorescence distribution for the cell shocked to 1.32 Osm (500 mM NaCl) was prevalent for > 15 min. The scale bar is 2 μm.

0.57 and 1.32 Osm, respectively), and Fig. 6B shows the corresponding confocal images. Cells shocked with up to 0.57 Osm showed a uniform distribution prior and after the measurement, as can be clearly seen from both the curves (Fig. 6A, ▲ and ●) and the confocal images (Fig. 6B). At 0.57 Osm and higher osmolalities, plasmolysis was observed, as could be seen from the cells no longer being ellipsoid shaped (Fig. 6B). Cells shocked with higher than 0.57 Osm of NaCl showed no longer a uniform distribution of GFP, and this non-uniform distribution was stable for >15 min (Fig. 6B). Note that for the cell in Fig. 6B shocked to 1.32 Osm (0.5 M NaCl), roughly half the cell was photo-bleached, a phenomena that was frequently observed for cells exposed to this high osmolality; in other cells we observed multiple unbleached spots. Importantly, the photo-bleached region was broader than can be expected on the basis of the radius of the focused laser beam (Airy disk, Fig. 6A), indicating that part of the GFP was still mobile (albeit slowed) but could not freely diffuse through the entire cell.

Figure 7A shows the average fluorescence distributions as a function of distance to the focused laser beam for ~30 cells, exposed to different salt concentrations. Clearly, the threshold for the apparent confinement of GFP to discrete pools in the cell was between 0.57 and 1.32 Osm. For cells shocked with NaCl to 1.32 Osm, the presence of K^+

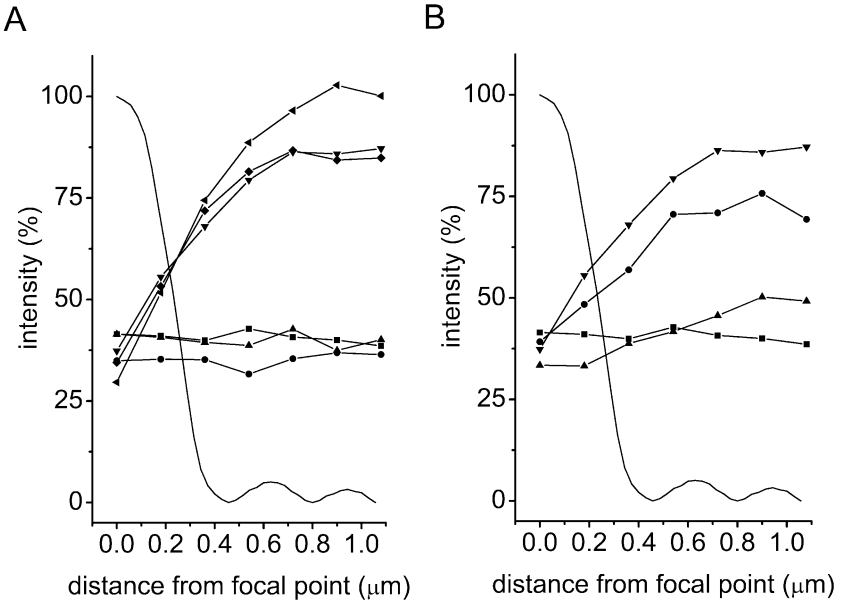

Fig. 7. A. The average fluorescence distributions as described in Fig. 1A for ~30 cells treated with NaCl. The fractions of cells that did not show a uniform distribution after photo-bleaching are indicated between the brackets: 0.15 Osm (0 M, ■, 0%), 0.37 Osm (125 mM, ▲, 0%), 0.57 Osm (250 mM, ●, ~5%), 1.32 Osm (500 mM, ▼, ~75%), 1.84 Osm (750 mM, ◆, ~100%) and 2.42 Osm (1 M, ◀, ~100%).
B. Unstressed cells at 0.15 Osm (■, 0%) and cells stressed to 1.32 Osm (500 mM NaCl, ▼, ~75%). The addition of 10 mM KCl (●, ~55%) or 10 mM KCl plus 1 mM glycine betaine and 1 mM proline (▲, ~20%) to the osmotically stressed cells resulted in (partial) restoration of the protein mobility. The bin width was 180 nm.

plus proline and glycine betaine led to almost full restoration of the mobility and the GFP was uniformly distributed through the cell (Fig. 7B). Importantly, when cells were transiently (5 min at 37°C) exposed to 1.32 Osm (500 mM NaCl) and subsequently diluted back to 0.15 Osm, only ~15% displayed a non-uniform distribution of GFP after photo-bleaching, and the mobility was the same as in unshocked cells. Decreasing the osmolality back to 0.15 Osm of cells that were stressed with a higher concentration of salt (1 M NaCl, 2.42 Osm) also resulted in a similar restoration of the mobility and about 15% of the cells had discrete pools of GFP. Dilution series of the untreated and osmotically shocked *E. coli* cells were plated on LB agar plates to determine the viability of the cells. For salt concentrations up to 1.32 Osm, the cells remained fully viable under the conditions used in this work. For higher concentrations, the viability decreased to 75 ± 10%, which is in accordance with published data, using similar but not identical media and stress conditions (Poirier *et al*., 1998; Konopka *et al*., 2006).

Discussion

Diffusion in bacterial cells

In this work, we used a combination of continuous photobleaching and FRAP to probe GFP diffusion in the cytoplasm of *E. coli*. Similar to the published FRAP studies (Elowitz *et al*., 1999; Konopka *et al*., 2006; Mullineaux *et al*., 2006), in our data analysis, we assume that the diffusion of GFP in the cytoplasm of *E. coli* obeys the Einstein-Stokes equation. However, diffusion in complex and crowded media has been reported to be anomalous (Metzler and Klafter, 2003), with the mean square displacement proportional to t^{α}, with the time factor $\alpha < 1$. Anomalous diffusion arises from interactions of the particle with its medium and has been observed in both eukaryotic (Tolic-Nørrelykke *et al*., 2004; Weiss *et al*., 2004) and prokaryotic (Golding and Cox, 2006) organisms. In *E. coli*, the diffusion of an mRNA-protein particle of ~100 nm has been reported to be anomalous with α about 0.7. However, as also indicated in (Golding and Cox, 2006), α is expected to be close to 1 for smaller particles such as GFP and the diffusion might be approximated by Brownian motion. Because there are no data available on anomalous diffusion of proteins in the cytoplasm, we did not incorporate this factor into our model. Because of this uncertainty, the diffusion constants should be regarded as apparent values, reflecting the speed of the particles for timescales of ~1 s (time of a laser pulse) and distances of ~400 nm (full width at half maximum).

Pulsed-FRAP measurements showed that GFP diffused in the cytoplasm of *E. coli* cells with an apparent diffusion constant D of 3.2 $\mu m^2 s^{-1}$ ($n = 64$) and ranging from 0.1 to 24 $\mu m^2 s^{-1}$. D did not correlate with the level of GFP expression (variation > 10-fold, Fig. 3B), contrary to what has been reported by Elowitz *et al*. (1999). This might be due to differences in the expression level or the FRAP method (see below). The measured diffusion constant is much lower than that of GFP in water [87 ± 2 $mm^2 s^{-1}$ (Potma *et al*., 2001)], and in the cytoplasm of most eukaryotic cells [27 $\mu m^2 s^{-1}$ in Chinese hamster ovary cells (Swaminathan *et al*., 1997)], which is consistent with the higher molecular crowding in bacteria. The diffusion constants obtained by pulsed-FRAP are in good agreement with the whole-cell FRAP measurements, where values of 8.2 ± 1.3 $\mu m^2 s^{-1}$ ($n = 21$, in *E. coli* MC1061) (Elowitz *et al*., 1999) and 6.2 ± 2.4 $\mu m^2 s^{-1}$ ($n = 39$) (Konopka *et al*., 2006) have been observed. Also, in these studies, a broad distribution of the diffusion constants, ranging from 1 to 15 $\mu m^2 s^{-1}$, has been reported (Elowitz *et al*., 1999; Konopka *et al*., 2006). Our value also agrees well with diffusion constants reported in the literature for other proteins in the *E. coli* cytoplasm. In cephalexin-elongated cells, a diffusion constant of $D = 9.0 \pm 2.1$ $\mu m^2 s^{-1}$ ($n = 6$) has been observed for the 30 kDa TorA-GFP fusion protein (Mullineaux *et al*., 2006), and $D = 2.5 \pm 0.6$ $\mu m^2 s^{-1}$ ($n = 8$) for the 72 kDa cMBP-GFP fusion protein (Elowitz *et al*., 1999). By means of FCS, $D = 4.6 \pm 0.8$ $\mu m^2 s^{-1}$ has been measured for the 40 kDa CheY-GFP fusion protein (Cluzel *et al*., 2000).

Osmotic stress in E. coli

Osmotically stressing *E. coli* cells from 0.15 to 0.6 Osm with NaCl (0.57 Osm, 250 mM) or sorbitol (0.62 Osm, 500 mM) led to a ~10-fold decrease in the intracellular GFP diffusion constant (Fig. 5, Table 1). Higher osmolalities resulted in part of the GFP becoming confined to discrete pools. Sorbitol and NaCl withdraw water from the cell (Poirier *et al*., 1998), thereby increasing the molecular crowding and viscosity and slowing down the diffusion. Glycerol showed no effect on the intracellular diffusion. Unlike sorbitol and NaCl, glycerol can rapidly enter the cell by either passive diffusion through the membrane (van der Heide *et al*., 2001) or via aquaglyceroporins, including the glycerol facilitator GlpF (Lu *et al*., 2003), and therefore only transiently withdraws water from the cell (that is, only shortly after addition of glycerol).

K^+ ions, glycine betaine and proline are rapidly accumulated by the cell upon osmotic shock (see Wood, 1999; Sleator and Hill, 2002 for reviews) and thereby preserve the water content of the cell. The presence of these osmoprotectants increased the mobility of GFP in the osmotically stressed cells (Figs 5B and 7B). Upon addition of K^+ ions in the absence of glycine betaine and proline, the diffusion constant was not fully restored and this is in good agreement with the finding that the presence of potassium does only lead to partial restoration of the water content

and cell volume (Cayley and Record, 2003). For osmoadaptation of *E. coli*, the uptake of glycine betaine and proline has priority over the accumulation of K^+ (and synthesis of glutamate and trehalose) as osmoprotectant (Dinnbier *et al*., 1988). *E. coli* has been shown to be able to grow over a 100-fold concentration range of NaCl, from 0.03 Osm (~15 mM) to 3 Osm (~1.5 M) (Cayley and Record, 2004). The growth rate, however, decreased linearly with salt concentrations above 0.28 Osm (~124 mM NaCl) (Cayley and Record, 2003), and the decreased protein diffusion constant might be an important parameter for this decline. Owing to the size exclusion principle, the decrease of the mobility can be expected to be even more pronounced for larger proteins (Spitzer and Poolman, 2005).

Cells upshocked with osmolalities higher than 0.6 Osm showed plasmolysis (Fig. 6B); the shape of these cells was no longer ellipsoid. In accordance with Konopka *et al*. (2006), plasmolysing cells showed slowed GFP diffusion but with our experimental setup it was not possible to quantify the extent of plasmolysis accurately. In fact, when the cells were osmotically shocked to 1.32 Osm or higher osmolalities, the GFP was no longer uniformly distributed. GFP became hindered in its diffusion from one end to the other end of the cell (Fig. 7). This non-uniform distribution of GFP was persistent for >15 min and the apparent diffusion constant for movement from one pool to another must have been lower than 0.001 $\mu m^2\ s^{-1}$ (with $D \approx l^2/t$). Because the region that was photo-bleached is much broader than the full width at half maximum of the laser (Figs 6A and 7), the diffusion of GFP within each pool must still have occurred with a reasonable rate. This leads to the important conclusion that moderate to severe hyperosmotic stress leads to compartmentalization of the cytoplasm into pools where the mobility of the GFP is still relatively high (only ~10-fold lower than in unshocked cells) but diffusion between pools is essentially absent.

Comparison of methods

The conclusions from this work differ from those of Konopka *et al*. (2006). It is therefore of particular importance to compare our approach to measure protein mobility with the one used in (Konopka *et al*., 2006) and to evaluate the two data sets. Although the baseline diffusion is very similar in both studies (D is 3.2 and 6.2 $\mu m^2\ s^{-1}$ respectively), Konopka *et al*. report a decrease in GFP mobility of up to three orders of magnitude (down to 0.01 $\mu m^2\ s^{-1}$) when the osmolality was increased from 0.24 to 0.94 Osm. This may seem contradictory with our findings, where the diffusion decreased ~10-fold only and this value was reached already when the osmolality was increased from 0.15 to 0.57 Osm (Fig. 5B). However, these apparent differences can be rationalized when the two methods are compared. In the study of Konopka *et al*. (Konopka *et al*., 2006), the diffusion of cytoplasmic GFP was measured by whole-cell FRAP, a method first used by Elowitz *et al*. (Elowitz *et al*., 1999). In (Konopka *et al*., 2006), a large part of the cell was bleached with a focused laser (full width at half maximum of 0.9 μm). Subsequently, time series of whole cell fluorescence images were recorded. These images were then converted to a one-dimensional intensity distribution, by averaging the fluorescence intensities perpendicular to the cell axis. The curves obtained were fitted with a model derived from Fick's diffusion equation. Because the fluorescence of the whole cell is taken into account, immobile or discrete pools of GFP (for instance as a consequence of hyperosmotic stress) contribute to the overall diffusion coefficient. Thus, the (low) diffusion coefficients probably reflect the presence of both mobile and immobile GFP. With pulsed-FRAP, however, a smaller part of the cell (in our case, the full width at half maximum is ~0.4 μm) is photo-bleached and the recovery of fluorescence in a discrete region allows heterogeneities to be observed. By plotting the percentage of fluorescence after the measurement as a function of distance from the laser beam (Fig. 1A, right panel), which is similar to the conversion of the cell image to the fluorescence intensity curve in (Konopka *et al*., 2006), we observed photo-bleaching in only a part of the cell. However, the photo-bleached region was larger than could be expected from the full width at half maximum of the focused laser beam (Fig. 6B). Parts of the cell showed no, or only very little, photo-bleaching and this non-uniform GFP distribution was prevalent for > 15 min. Therefore, in cells shocked with a high osmolality, discrete pools of GFP must exist. For cells stressed at lower osmolalities (≤ 0.6 Osm), we cannot rule out the possibility that transient pools of GFP exist, which must then be smaller than the ~400 nm spatial resolution of the measurements. The large spread of the diffusion constants might reflect such cytoplasmic heterogeneities. If such pools would exist, the diffusion between them must be high, because the apparent diffusion of GFP in the cytoplasm of *E. coli* at low osmolality was 0.4–3.2 $\mu m^2\ s^{-1}$.

In addition to the whole cell image analysis (Elowitz *et al*., 1999; Konopka *et al*., 2006; Mullineaux *et al*., 2006), conventional FRAP measurements were performed on organelles of similar size as a bacterial cell, most notably mitochondria (Dinnbier *et al*., 1988; Partikian *et al*., 1998). In these studies, GFP was photobleached by a focused laser beam at high intensity. Subsequently, the redistribution of GFP and GFP fusion proteins in the mitochondrial lumen was monitored using an attenuated probe beam. The half recovery time $t_{1/2}$ was taken from the curve, which was then converted into a diffusion constant by using a complex mathematical model (Ölveczky and Verkman, 1998; Partikian *et al*.,

1998; Haggie and Verkman, 2002) to account for the orientation and geometry of the mitochondria. In principle, the diffusion of GFP in bacteria could be measured using a similar approach. However, it would be difficult to convert $t_{1/2}$ to a diffusion coefficient, because additional photo-bleaching by the attenuated probe beam is relatively high due to the photo-instability of the bacterial GFP used. Furthermore, due to our small probe beam diameter (Fig. 1A, dotted circle), the assumption of one-dimensional diffusion cannot be made (as in Partikian *et al*., 1998; Elowitz *et al*., 1999; Haggie and Verkman, 2002; Konopka *et al*., 2006; Mullineaux *et al*., 2006). Also, in our case, the orientation and geometric shape of the bacteria is precisely known because the cells were immobilized on the poly-L-lysine-coated cover glass and a confocal image of the cell was recorded. Therefore, a numerical approach as described in this study is preferred over an analytical model. This numerical approach has further advantages that more complex geometries of the cell and beam profile can be easily taken into account.

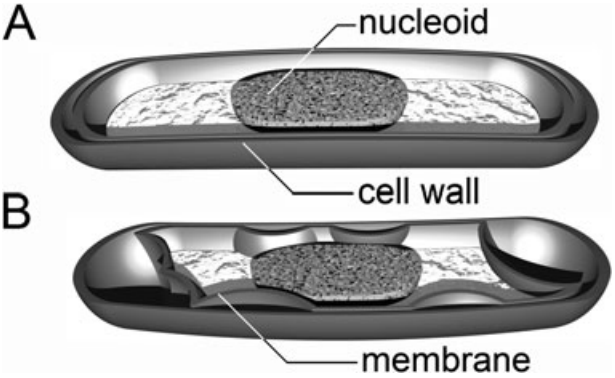

Fig. 8. Cartoon to illustrate the effect of hyperosmotic stress on the proposed compartmentalization of the cell.
A. Cell exposed to no or low (up to 0.6 Osm) osmotic stress.
B. Cell exposed to moderate or severe osmotic stress (> 0.6 Osm). Under these conditions, the cell membrane is proposed to contact the nucleoid, which results in a diffusive barrier and discrete pools of GFP.

Physiological relevance of slowed diffusion

What causes part of the GFP to become immobile? It has been speculated that the cytoplasm forms a biopolymer meshwork comprising of the nucleoid with proteins, RNA, ribosomes and associated water (Spitzer and Poolman, 2005), in which protein might get trapped at high osmotic stress (Gitai, 2005). Aggregation due to chaotropic effects is unlikely, because the mobility is restored after diluting osmotically shocked cells back to 0.15 Osm. The nucleoid consists of the highly compressed genome and associated proteins into one or two discrete bodies, which occupy about 1/4 of the intracellular volume of the cell (for a review see Zimmerman, 2006). It is tempting to speculate that owing to the hyperosmotic stress, the cell membrane is pushed against a compacted nucleoid, thereby forming a barrier in the cell that hinders macromolecule diffusion and results in separated pools of GFP (Fig. 8).

The maximum decrease of the protein mobility was reached after an increase of the osmolality from 0.15 to 0.6 Osm (Fig. 5A). This observation is in accordance with measurements of cytoplasmic water, which decreases linearly up to osmolalities of 1 Osm (Cayley *et al*., 1991). At this point, the cytoplasmic water attained a constant value of 0.5 g H_2O g^{-1} cytoplasmic macromolecules, corresponding to the amount of water 'bound' to macromolecules (Cayley *et al*., 1991). Thus, only a certain amount of water can be abstracted from the cell (the 'free, bulk-like' water) and this leads to the lower protein mobility. Further addition of salt leads to compartmentalization of GFP, probably via the formation of diffusive barriers and/or formation of a biopolymer meshwork (Spitzer and Poolman, 2005; Gitai, 2005). Upon long-term exposure to hyperosmotic stress, the proteins may ultimately aggregate and cause loss of viability. On the assumption that *E. coli* is rod-shaped, we were able to calculate from the confocal images the volume of each of the cells (Fig. 3C). Upon an increase of the osmolality from 0.15 to 0.57 Osm, the average cell volume decreased from 2.9 ± 1.3 fl to 1.8 ± 1.1 fl, in accordance with (Cayley *et al*., 1991). The spread in the cell volumes is relatively large due to variations in cell sizes of the bacteria. The decrease in the cell volume was mainly due to changes of the cell length; the cell diameter was 1.0 ± 0.3 μm and decreased to 0.9 ± 0.3 μm upon an osmotic increase. Higher osmotic upshocks did not result in a significant further decrease of the cell volume. When cells were shocked for 5 min with up to 2.42 Osm and subsequently were diluted back to 0.15 Osm, the protein mobility was almost completely restored and only ~15% of the cells contained an immobile fraction. Importantly, this number coincided with the viability of the cells, suggesting that the cells, where the protein diffusion was not restored, were not viable. Osmotically stressing the cells for longer times is likely to decrease the viability further.

Verkman *et al*. (Kao *et al*., 1993) studied the effects of osmotic shocks on the mobility of low molecular weight fluorophores such as BCECF in eukaryotic fibroblasts. A decrease of the cell volume of threefold led to a sixfold decrease of the diffusion coefficient of BCECF. Because the sizes of the probes (0.5 kDa for BCECF and 2×26 kDa for dimeric GFP) and the internal (crowding) conditions (Cayley *et al*., 1991; Zimmerman and Trach, 1991; Cayley and Record, 2004) in the cells are very different, a comparison of these data with our work may not be justified.

Variation in diffusion constants

The spread in the diffusion constants was relatively large (Fig. 5, Table 1), and is somewhat larger than reported in the literature (Elowitz *et al*., 1999; Konopka *et al*., 2006; Mullineaux *et al*., 2006). This might be partly attributed to experimental errors and partly to true physiologically relevant variations. Experiments with a viscous (~90 mPa s, Fig. 4) homogeneous mixture encapsulated into giant liposomes showed that pulsed-FRAP enables to obtain reasonably accurate diffusion constants, with a standard deviation of ~75%. Multiple measurements on the same position in a bacterial cell confirm this error, which is probably due to the contribution of out of focus light, the estimation of the cell cross-sectional area and distortions of the laser beam profile. The error of the method, however, is much smaller than the variation in the data obtained from different bacterial cells. The larger variation in diffusion coefficients in the *in vivo* experiments must thus be due to true biological variations and possibly the positioning of the laser beam relative to the nucleoid (see previous paragraph).

To further compare the accuracy of pulsed-FRAP with whole-cell FRAP (Elowitz *et al*., 1999; Konopka *et al*., 2006; Mullineaux *et al*., 2006), GFP diffusion measurements in cephalexin-treated cells were repeated with pulsed-FRAP. A diffusion constant of $9.8 \pm 3.6\ \mu m^2\ s^{-1}$ was found. This error is also somewhat larger than reported in the literature [$D = 8.2 \pm 1.3\ \mu m^2\ s^{-1}$ (Elowitz *et al*., 1999), $D = 9.0 \pm 2.1\ \mu m^2\ s^{-1}$ (Mullineaux *et al*., 2006)] and this indicates that our method is somewhat less precise than whole-cell FRAP. With pulsed-FRAP, only fluorescence from the position of the focused laser is taken into account (Fig. 1B), whereas whole-cell FRAP uses information from the whole cell (Elowitz *et al*., 1999; Konopka *et al*., 2006; Mullineaux *et al*., 2006). Thus, with pulsed-FRAP, the diffusion of GFP is measured at a certain position of the cell and only fluorophores at that position are observed. The cytoplasm is highly heterogeneous, for instance due to the presence of the nucleoid, and the positioning of the laser beam relative to nucleoid will be a cause of variation in the diffusion coefficients. The nucleoid is likely to have different permeability and viscosity properties than the rest of the cell (Zimmerman, 2006). It has been reported that the nucleoid affects the diffusion of mRNA (Golding and Cox, 2006). The packing of the nucleoid is also dependent on the stages of the cell cycle and could thus affect the intracellular protein mobility (Zimmerman, 2006). We consider it unlikely that the spread in diffusion constants in the unstressed cells is caused by a population of immobile or aggregated GFP, because the initial fluorescence was spatially uniform (Fig. 6B) and no GFP inclusion bodies were observed by microscopy. Moreover, if GFP ended up in inclusion bodies, the protein would not be fluorescent (Waldo *et al*., 1999). The advantage of pulsed-FRAP over whole-cell FRAP is that discrete pools of fluorophores can be discriminated. In the future, we aim to use this feature of pulsed-FRAP to further delineate the cytoplasmic heterogeneity.

Apparent viscosity of the cytoplasm

Assuming a Stokes radius of 3.5 nm for a monodisperse globular protein of 52 kDa (for dimeric GFP, 2.8 nm for monomeric) (Terry *et al*., 1995), the apparent viscosity in the cell can be calculated with the Einstein-Stokes relationship. However, the Einstein-Stokes relationship assumes (i) a solution with a constant viscosity and (ii) constant interactions between the moving particle and the solvent. In a cell, none of these assumptions is valid, and the calculated viscosity can thus only be regarded as an indication of the crowdedness inside the cell (Table 1). In the cytosol of eukaryotic cells, assuming a diffusion constant of $27\ \mu m^2\ s^{-1}$ for GFP (Swaminathan *et al*., 1997), the apparent viscosity is 3 mPa s, three times higher than that of water (0.9 mPa s). For *E. coli* cells at 0.15 Osm, this value is 25 mPa s ($D = 3.2\ \mu m^2\ s^{-1}$). Upon an increase of the osmolality to 0.57 Osm ($D = 0.4\ \mu m^2\ s^{-1}$), this value increases to 197 mPa s, which is roughly 200 times that of water. Any diffusion-limited processes in the cell, e.g. reactions requiring macromolecular association-dissociating steps, will be slowed in such osmotically stressed cells.

Concluding remarks

This study shows the impact of osmotic stress on the mobility of proteins in the cytoplasm of *E. coli*. At a medium osmolality of 0.15 Osm, GFP diffused through the cytoplasm of *E. coli* cells with a diffusion coefficient of D $\sim 3.2\ \mu m^2\ s^{-1}$. Shifting the cells to a medium of 0.6 Osm resulted in a ~10-fold decrease of the diffusion coefficient. At higher osmolalities and in the absence of osmoprotectants, discrete pools of GFP were observed and the diffusion between these pools was very low (apparent D of < 0.001). By mapping the diffusion at the poles and at the nucleoid, we may be able to elucidate the diffusional barriers and better understand the impact of molecular crowding in the cell.

With pulsed-FRAP, the cell size and shape are taken into account and this enables one to measure the diffusion of molecules in small bacterial cells and eukaryotic organelles that cannot be assessed by means of standard microscopy methods. In pulsed-FRAP, only a very small fraction of the fluorophore is photo-bleached, allowing multiple measurements to be performed in the same cell. It also enables diffusion measurements with relatively photo-unstable fluorophores. In the future, we aim to apply pulsed-FRAP for measurements of diffusion of other

biomacromolecules, differing in size and surface properties, and small fluorophores.

Experimental procedures

Sample preparation

Escherichia coli strain MC1061 (Belgian Coordinated Collections of Microorganisms accession no. LMBP 472, *Δ(araA-leu)7697 araD139 Δ(codB-lac)3 Δlac74 galK16 galE15 mcrA0 relA1 rpsL150 spoT1 mcrB9999 hsdR2 λ⁻F⁻*) (Casadaban and Cohen, 1980) was transformed with pGFPCR (National Center for Biotechnology Information accession no. AF007834) (Cormack and Somssich, 1997). The pGFPCR plasmid is a derivative of pGFPuv (Clontech) and carries the cycle 3 variant of GFP (Crameri *et al*., 1996) behind the *lac* promoter. GFP has a tendency to dimerize, and, at the expression levels used, it is likely we studied the diffusion of dimers (Konopka *et al*., 2006). The cells were grown aerobically to exponential phase (OD at 660 nm of 0.2–0.5) at 37°C in LB medium supplemented with ampicillin (50 μg ml^{-1}), but without inducer to keep the level of GFP relatively low. Cells were then harvested and washed three times to reach an optical density at 660 nm of 0.5 in either 25 mM or 200 mM sodium phosphate, pH 7.0, each supplemented with 50 mM glucose. The cells were kept on ice prior to the measurements. The osmolality of the media was measured by determination of the freezing point, using a Osmomat 030 (Gonotec GmbH, Berlin, Germany).

After incubation of 10 μl of cell suspension for 5 min at 37°C, a 50 times excess of fresh medium (preheated at 37°C) was added as specified in Table 1, that is, with or without 10 mM K^+, 1 mM proline and/or 1 mM glycine betaine. After additional 5 min incubation at 37°C, a microscope sample was prepared by applying 10 μl on a poly-L-lysine-coated cover glass. The poly-L-lysine prevented the cell from moving and a comparison of cell images prior and after each measurement indicated that the cells were completely immobilized. Because the sample consisted of a small volume and low cell density, the oxygen content of the sample was assumed constant. At the GFP expression levels used, the contribution of the autofluorescence to the total signal was insignificant. The diffusion of GFP inside the cells was measured at room temperature.

Preparation of giant liposomes

A mixture of PEG6000 and isolated cytosol from *E. coli* cells, expressing GFP, was encapsulated into ~μm-sized liposomes. Cells in the late exponential phase of growth from a 1 l culture were washed and resuspended in 3 ml milli-Q containing tracer amounts of deoxyribonuclease 1 (Sigma, St. Louis, MO). Cell lysis was achieved by sonification at 30 W with the instrument (Vibra Cell V91301, Bioblock Scientific, Illkirch, France) in pulse modus (15 periods of 15 s on – 45 s off) on ice. Unbroken cells and membranes were removed by centrifugation (300 000 *g*, 10 min). The supernatant was mixed 1:1 with a solution of 400 g PEG6000 kg^{-1} milli-Q. The viscosity of this mixture was ~90 mPa s, which is similar to the estimated viscosity of the cytoplasm inside the *E. coli* cell (see *Discussion* section).

The cytoplasm/PEG6000 mixture was encapsulated in ~μm-sized liposomes as described by Pautot *et al*. (2003) and Noireaux and Libchaber (2004). Briefly, inverted micelles were created by suspending 0.8 mg ml^{-1} of a 3:1 mixture of DOPG/DOPC in dodecane by 30 min sonification in a cleaning sonic bath and overnight stirring at 30°C. Subsequently, 1 μl of the cytoplasm/PEG6000 mixture was added to 50 μl of the emulsion and small droplets of ~μm size were created by vortexing for 30 s. The lipid dispersion was then placed on top of 100 μl of 50 mM potassium phospate, pH 7.0, and the sample was centrifuged for 10 min at 200 *g*. During the centrifugation, the water droplets migrated from the dodecane to the aqeuous phase and liposomes were formed.

Optical setup

Measurements of the diffusion coefficients were carried out on a laser scanning confocal microscope (Doeven *et al*., 2005), based on an inverted microscope Axiovert S 100 TV (Zeiss, Jena, Germany), in combination with a galvanometer optical scanner (model 6860, Cambridge Technology, Watertown, MA) and a microscope objective nano-focusing device (P-721, PI). For excitation of GFP, an argon ion laser (488 nm, Spectra-Physics) was directed through an electronic shutter (Melles Griot) and was focused by a Zeiss C-Apochromat infinity-corrected 1.2 NA 63× water immersion objective. The intensity of the laser did not exceed 10 μW at the back aperture of the objective. The lateral radius ω, defined as the point where the fluorescence count rate per molecule decreased e^2 times was 180 nm. Emission was collected through the same objective, separated from the excitation beam by a beam pick-off plate (BSP20-A1, ThorLabs), and directed through an emission filter (HQ 535/50, Chroma Technology) and a pinhole (diameter of 30 μm) onto an avalanche photodiode (SPCM-AQR-14, EG and G). The fluorescence signal was digitized and acquired by a PC.

Data analysis

The fluorescence is linearly proportional to the GFP concentration and changes in time due to diffusion and photobleaching of GFP. Considering the elongated shape of the confocal volume, the motion of GFPs in *E. coli* can be approximated to be two-dimensional (in lateral directions, r) as in (Elowitz *et al*., 1999; Mullineaux *et al*., 2006; Konopka *et al*., 2006). GFP is initially ($t \leq t_0$, Fig. 1B) uniformly distributed in the cell and has concentration C_0. Assuming that GFP diffusion obeys the classic Brownian motion law with a single diffusion constant D (see *Discussion* section), Fick's second law can be applied for the GFP concentration fluctuations inside the cell $C(r, t)$:

$$\frac{\delta C(r,t)}{\delta t} = D\Delta C(r,t) \quad (1)$$

Secondly, we assume that the photo-bleaching rate is proportional to the intensity of the focused laser beam $I(r)$:

$$\frac{\delta C(r,t)}{\delta t} = BI(r)C(r,t) \quad (2)$$

where B is a bleaching constant. Based on these assumptions, diffusion constant D and bleaching constant B were obtained from the fluorescence traces (Fig. 1B) in the following way: A computational grid was superimposed over the confocal images of the bacterium (Fig. 1A, left panel), with x and y grid indices i and j, respectively, and grid spacing r_s. At the membrane of the bacterium, Neumann boundary conditions [$\nabla C(r, t) = 0$] were assumed and the concentration of GFP at each grid point was calculated using an explicit finite difference method with time step t_s:

$$C_{i,j,t+t_s} = C_{i,j,t} + \frac{Dt_s}{r_s^2}[C_{i+1,j,t} + C_{i-1,j,t} + C_{i,j+1,t} + C_{i,j-1,t} - 4C_{i,j,t}] - t_s B_{i,j,t} \quad (3)$$

where $B_{i,j,t}$ is the decrease of the fluorescence due to photobleaching. This method is numerically stable and convergent when $D \cdot t_s / r_s^2 < 0.25$ and the time steps and grid spacing should be chosen accordingly. For GFP in *E. coli*, diffusion coefficients are typically smaller than 20 $\mu m^2\ s^{-1}$ (Elowitz *et al*., 1999; Konopka *et al*., 2006; Mullineaux *et al*., 2006), and t_s and r_s were 50 μs and 100 nm respectively. Because the intensity of a focused laser beam follows a Gaussian distribution perpendicular to the optical axis (in r):

$$B_{i,j,t} = BI_{i,j}C_{i,j,t} \quad (4)$$

$$I_{i,j} = \exp\left(-\frac{r_s^2}{\omega^2}\left((i - i_0)^2 + (j - j_0)^2\right)\right) \quad (5)$$

where (i_0, j_0) is the position of the focused laser beam (Fig. 1A, left panel). After a certain bleaching time, at $t = t_1$ (Fig. 1B), the detected fluorescence has decreased to:

$$C_1 = \sum_{i,j} I_{i,j} C_{i,j,t_1} \quad (6)$$

where the summation is over all the grid points that are located in the bacterium. At this time, the shutter is closed for a time period long enough to allow redistribution of the remaining GFP ($t = t_2$, Fig. 1B). After this time interval, the shutter is opened and the fluorescence is again measured for 1 s. Because (mobile) GFP has been homogenously distributed in the cell and the total amount of GFP in the cell did not change between t_1 and t_2 (no photo-bleaching):

$$C_2 = \sum_{i,j} I_{i,j} \sum_{i,j} \frac{C_{i,j,t_1}}{N} \quad (6)$$

where N is the number of grid points that are located in the bacterium.

In brief, a diffusion measurement consists of the following steps: First, a confocal image of the bacterium is recorded (Fig. 1A, left panel). Then, the laser beam is focused in the cell (at position (i_0, j_0), Fig. 1A) and 5–15 laser pulses are applied with varying interval times. After each measurement, a second confocal image is recorded to check whether the fluorescence is distributed uniformly. Subsequently, a computational grid is superimposed over the confocal image (Fig. 1A, left panel) and the decrease of C(t) is modelled for different combinations of B and D, using Eqs 3–6. Using multivariate least square statistics, the fluorescence intensity measurements are then fitted by minimizing $\{[C(t)/C_0]^{measured} - [C(t)/C_0]^{modeled}\}^2$, using a program written in Visual Basic.NET.

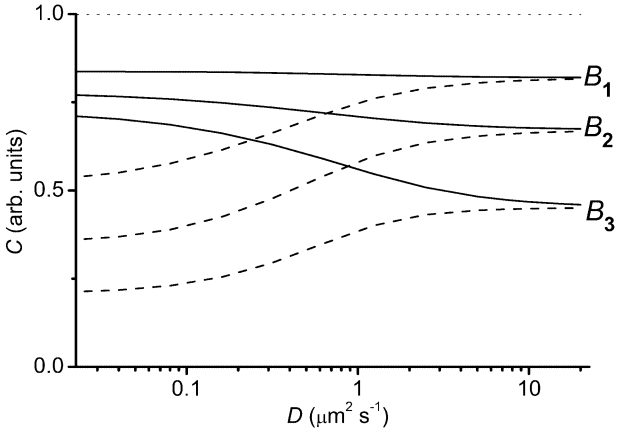

Fig. 9. Dynamic range of pulsed-FRAP measurements. C_0 (dotted line) was set to 1, and C_1 (dashed line) and C_2 (solid line) were calculated for a typical *E. coli* cell of 3.2 × 0.8 μm, using Eqs 3–6 and bleaching rates of $B_1 = 2.5\ s^{-1}$, $B_2 = 5\ s^{-1}$ and $B_3 = 10\ s^{-1}$.

To estimate the dynamic range of the method, the diffusion constant D versus C_0, C_1 and C_2 were plotted for different bleaching constants of a typical rod-shaped *E. coli* bacterium of 3.2 × 0.8 μm (Fig. 9). As can be seen from the figure, the range of the diffusion constants that is accessible with this method lies between 0.01 and 20 $\mu m^2\ s^{-1}$. For diffusion coefficients larger than 20 $\mu m^2\ s^{-1} C_2 - C_1 \rightarrow 0$, and due to fast protein motion the whole cell is photo-bleached instantly. By decreasing the photo-bleach time (from t_0 to t_1, Fig. 1B), faster diffusion can in principle be measured, although r_s and t_s should be decreased accordingly to keep $D \cdot t_s / r_s^2 < 0.25$. For diffusion coefficients smaller than 0.01 $\mu m^2\ s^{-1}$, the decay in fluorescence becomes too small to allow for accurate determination of the diffusion coefficient. The dynamic range of D for smaller and for larger cells shifts to lower and higher values respectively. For very large cells (> 10 μm), $C_0 - C_1 \rightarrow 0$, and the diffusion constant cannot be determined accurately. However, for cells of this size conventional FRAP or FCS can be used.

In general, FCS requires a low number of particles in the detection volume (0.1–100 nM), whereas FRAP-based techniques, such as pulsed-FRAP, are more applicable for higher concentrations of fluorophore. For photo-unstable fluorophores, the diffusion can be accessed with pulsed-FRAP, whereas FCS and conventional FRAP require more photostable dyes. For diffusion in small, μm-sized compartments fitting of FRAP and fluorescence autocorrelation curves is challenging, due to the influence of nearby membranes (Fradin *et al*., 2003). Because the cell size and shape are taken into account in the pulsed-FRAP method, this procedure enables to measure diffusion in very small compartments.

Acknowledgements

We thank Robert S. Cormack and Imre E. Somssich for kindly supplying the GFP construct and Sytse A. Henstra for helpful advice. We are grateful to the Netherlands Science Foundation (NWO), ALW Grant number 814.02.002, and the Zernike Institute for Advanced Materials for financial support.

References

Casadaban, M.J., and Cohen, S.N. (1980) Analysis of gene control signals by DNA fusion and cloning in *Escherichia coli*. *J Mol Biol* **138:** 179–207.

Cayley, S., and Record, M.T., Jr (2003) Roles of cytoplasmic osmolytes, water, and crowding in the response of *Escherichia coli* to osmotic stress: biophysical basis of osmoprotection by glycine betaine. *Biochemistry* **42:** 12596–12609.

Cayley, S., and Record, M.T., Jr (2004) Large changes in cytoplasmic biopolymer concentration with osmolality indicate that macromolecular crowding may regulate protein-DNA interactions and growth rate in osmotically stressed *Escherichia coli* K-12. *J Mol Recognit* **17:** 488–496.

Cayley, S., Lewis, B.A., Guttman, H.J., and Record, M.T., Jr (1991) Characterization of the cytoplasm of *Escherichia coli* K-12 as a function of external osmolarity. Implications for protein-DNA interactions *in vivo*. *J Mol Biol* **222:** 281–300.

Cluzel, P., Surette, M., and Leibler, S. (2000) An ultrasensitive bacterial motor revealed by monitoring signaling proteins in single cells. *Science* **287:** 1652–1655.

Cormack, R.S., and Somssich, I.E. (1997) Cloning of PCR products via the green fluorescent protein. *Techn Tips Online* **1:** T01107.

Crameri, A., Whitehorn, E.A., Tate, E., and Stemmer, W.P. (1996) Improved green fluorescent protein by molecular evolution using DNA shuffling. *Nat Biotechnol* **14:** 315–319.

Delon, A., Usson, Y., Derouard, J., Biben, T., and Souchier, C. (2006) Continuous photo-bleaching in vesicles and living cells: a measure of diffusion and compartmentation. *Biophys J* **90:** 2548–2562.

Dinnbier, U., Limpinsel, E., Schmid, R., and Bakker, E.P. (1988) Transient accumulation of potassium glutamate and its replacement by trehalose during adaptation of growing cells of *Escherichia coli* K-12 to elevated sodium chloride concentrations. *Arch Microbiol* **150:** 348–357.

Doeven, M.K., Folgering, J.H., Krasnikov, V., Geertsma, E.R., van den Bogaart, G., and Poolman, B. (2005) Distribution, lateral mobility and function of membrane proteins incorporated into giant unilamellar vesicles. *Biophys J* **88:** 1134–1142.

Eberhardt, C., Kuerschner, L., and Weiss, D.S. (2003) Probing the catalytic activity of a cell division-specific transpeptidase *in vivo* with beta-lactams. *J Bacteriol* **185:** 3726–3734.

Ellis, R.J. (2001) Macromolecular crowding: obvious but underappreciated. *Curr Opin Struct Biol* **11:** 114–119.

Elowitz, M.B., Surette, M.G., Wolf, P.E., Stock, J.B., and Leibler, S. (1999) Protein mobility in the cytoplasm of *Escherichia coli*. *J Bacteriol* **181:** 197–203.

Fischer, E. (1989) Osmolability of *Escherichia coli* and modification of [125I]ampicillin-binding by competence induction for uptake of transforming DNA. *Arch Microbiol* **153:** 43–46.

Fradin, C., Abu-Arish, A., Granek, R., and Elbaum, M. (2003) Fluorescence correlation spectroscopy close to a fluctuating membrane. *Biophys J* **84:** 2005–2020.

Gitai, Z. (2005) The new bacterial cell biology: moving parts and subcellular architecture. *Cell* **120:** 577–586.

Golding, I., and Cox, E.C. (2006) Physical nature of bacterial cytoplasm. *Phys Rev Lett* **96:** 98–102.

Haggie, P.M., and Verkman, A.S. (2002) Diffusion of tricarboxylic acid cycle enzymes in the mitochondrial matrix *in vivo*. Evidence for restricted mobility of a multienzyme complex. *J Biol Chem* **277:** 40782–40788.

van der Heide, T., Stuart, M.C., and Poolman, B. (2001) On the osmotic signal and osmosensing mechanism of an ABC transport system for glycine betaine. *EMBO J* **20:** 7022–7032.

Ishihara, A., Segall, J.E., Block, S.M., and Berg, H.C. (1983) Coordination of flagella on filamentous cells of *Escherichia coli*. *J Bacteriol* **155:** 228–237.

Kao, H.P., Abney, J.R., and Verkman, A.S. (1993) Determinants of the translational mobility of a small solute in cell cytoplasm. *J Cell Biol* **120:** 175–184.

Konopka, M.C., Shkel, I.A., Cayley, S., Record, M.T., and Weisshaar, J.C. (2006) Crowding and confinement effects on protein diffusion *in vivo*. *J Bacteriol* **188:** 6115–6123.

Lippincott-Schwartz, J., Altan-Bonnet, N., and Patterson, G.H. (2003) Photobleaching and photoactivation: following protein dynamics in living cells. *Nat Cell Biol* **5:** S7–S14.

Lu, D., Grayson, P., and Schulten, K. (2003) Glycerol conductance and physical asymmetry of the *Escherichia coli* glycerol facilitator GlpF. *Biophys J* **85:** 2977–2987.

Metzler, R., and Klafter, J. (2003) When translocation dynamics becomes anomalous. *Biophys J* **85:** 2776–2779.

Mullineaux, C.W., Nenninger, A., Ray, N., and Robinson, C. (2006) Diffusion of green fluorescent protein in three cell environments in *Escherichia coli*. *J Bacteriol* **188:** 3442–3448.

Noireaux, V., and Libchaber, A. (2004) A vesicle bioreactor as a step toward an artificial cell assembly. *Proc Nat Acad Sci USA* **101:** 17669–17674.

Ölveczky, B.P., and Verkman, A.S. (1998) Monte Carlo analysis of obstructed diffusion in three dimensions: application to molecular diffusion in organelles. *Biophys J* **74:** 2722–2730.

Partikian, A., Ölveczky, B., Swaminathan, R., Li, Y., and Verkman, A.S. (1998) Rapid diffusion of green fluorescent protein in the mitochondrial matrix. *J Cell Biol* **140:** 821–829.

Pautot, S., Frisken, B.J., and Weitz, D.A. (2003) Engineering asymmetric vesicles. *Proc Nat Acad Sci USA* **100:** 10718–10721.

Poirier, I., Maréchal, P.-A., Evrard, C., and Gervais, P. (1998) *Escherichia coli* and *Lactobacillus plantarum* responses to osmotic stress. *Appl Microbiol Biotechnol* **50:** 704–709.

Potma, E.O., de Boeij, W.P., Bosgraaf, L., Roelofs, J., van Haastert, P.J., and Wiersma, D.A. (2001) Reduced protein diffusion rate by cytoskeleton in vegetative and polarized dictyostelium cells. *Biophys J* **81:** 2010–2019.

Sleator, R.D., and Hill, C. (2002) Bacterial osmoadaptation: the role of osmolytes in bacterial stress and virulence. *FEMS Microbiol Rev* **26:** 49–71.

Spitzer, J.J., and Poolman, B. (2005) Electrochemical structure of the crowded cytoplasm. *Trends Biochem Sci* **30:** 536–541.

Starka, J. (1971) Formation et stabilite osmotique des formes filamenteuses d'*Escherichia coli* induites par la penicilline. *Ann Inst Pasteur (Paris)* **121:** 149–159.

Swaminathan, R., Hoang, C.P., and Verkman, A.S. (1997) Photo-bleaching recovery and anisotropy decay of green fluorescent protein GFP-S65T in solution and cells: cytoplasmic viscosity probed by green fluorescent protein translational and rotational diffusion. *Biophys J* **72:** 1900–1907.

Terry, B.R., Matthews, E.K., and Haseloff, J. (1995) Molecular characterisation of recombinant green fluorescent protein by fluorescence correlation microscopy. *Biochem Biophys Res Commun* **217:** 21–27.

Tolic-Nørrelykke, I.M., Munteanu, E.-L., Thon, G., Oddershede, L., and Berg-Sørensen, K. (2004) Anomalous diffusion in living yeast cells. *Phys Rev Lett* **93:** 78–102.

Waldo, G.S., Standish, B.M., Berendzen, J., and Terwilliger, T.C. (1999) Rapid protein-folding assay using green fluorescent protein. *Nat Biotechnol* **17:** 691–695.

Weiss, M., Elsner, M., Kartberg, F., and Nilsson, T. (2004) Anomalous subdiffusion is a measure for cytoplasmic crowding in living cells. *Biophys J* **87:** 3518–3524.

Wood, J.M. (1999) Osmosensing by bacteria: signals and membrane-based sensors. *Microbiol Mol Biol Rev* **63:** 230–262.

Zimmerman, S.B. (2006) Shape and compaction of *Escherichia coli* nucleoids. *J Struct Biol* **156:** 255–261.

Zimmerman, S.B., and Trach, S.O. (1991) Estimation of macromolecule concentrations and excluded volume effects for the cytoplasm of *Escherichia coli*. *J Mol Biol* **222:** 599–620.

